Joint frailty modelling of time-to-event data to elicit the evolution pathway of events: A generalised linear mixed model approach

Journal:	*Biostatistics*
Manuscript ID	BIOSTS-20400
Manuscript Type:	Article
Date Submitted by the Author:	26-Nov-2020
Complete List of Authors:	Ng, Shu Kay (Angus); Griffith University, School of Medicine Tawiah, Richard; University of New South Wales, School of Psychology McLachlan, Geoffrey; University of Queensland, Department of Mathematics Gopalan, Vinod; Griffith University - GC Campus
Keywords:	Cancer registry data, Generalised linear mixed models, Informative censoring, Mean residual life, Multimorbidity, Secondary primary cancer

Biostatistics (2020), **0**, 0, *pp.* 1–25
doi:10.1093/biostatistics/output

Joint frailty modelling of time-to-event data to elicit the evolution pathway of events: A generalised linear mixed model approach

SHU-KAY NG*

School of Medicine and Menzies Health Institute Queensland, Griffith University, Australia

s.ng@griffith.edu.au

RICHARD TAWIAH

School of Psychology, University of New South Wales, Australia

GEOFFREY J. MCLACHLAN

Department of Mathematics, University of Queensland, Australia

VINOD GOPALAN

School of Medicine and Menzies Health Institute Queensland, Griffith University, Australia

Summary

Multimorbidity constitutes a serious challenge on the healthcare systems in the world, due to its association with poorer health-related outcomes, more complex clinical management, increases in health service utilisation and costs, but a decrease in productivity. However, to date most evidence on multimorbidity is derived from cross-sectional studies that have limited capacity to understand the pathway of multimorbid conditions. In this paper, we present an innovative perspective on analysing longitudinal data within a statistical framework of survival analysis of

*To whom correspondence should be addressed.

time-to-event recurrent data. The proposed methodology is based on a joint frailty modelling approach with multivariate random effects to account for heterogeneous risk of failure and the presence of informative censoring due to a terminal event. We develop a generalised linear mixed model (GLMM) method for efficient estimation of parameters. We demonstrate the capacity of our approach using a real cancer registry data set on the multimorbidity of melanoma patients and document the relative performance of the proposed joint frailty model to the natural competitor of a classical frailty model via extensive simulation studies. Our new approach is timely to advance evidence-based knowledge to address increasingly complex needs related to multimorbidity and develop interventions that are most effective and viable to better help the large number of individuals with multiple conditions.

Key words: Cancer registry data; Generalised linear mixed models; Informative censoring; Mean residual life; Multimorbidity; Secondary primary cancer.

1. Introduction

Recent editorial published in Lancet and the UK Academy of Medical Sciences in 2018 has identified multimorbidity as a priority for global research in health sciences (Lancet editorial, 2018; Academy of Medical Science, 2018). Multimorbidity, defined as the coexistence of two or more chronic conditions within a single patient (van den Akker *and others*, 1996), constitutes a serious burden and challenge on individuals and healthcare systems in many countries because of its association with poorer health-related outcomes, lower quality of life, increases in health service utilisation and costs, but a decrease in productivity (Di Angelantonio *and others*, 2015; Ng *and others*, 2019*b*; Pearson-Stuttard *and others*, 2019; Richardson *and others*, 2020). However to date most evidence on multimorbidity is derived from cross-sectional studies, focusing on identifying groups of multimorbid health conditions (Marengoni *and others*, 2009; Ng *and others*, 2012,

2018) or groups of individuals with different multimorbidity patterns (Ng, 2015; Ng *and others*, 2019*a*; Vanfleteren *and others*, 2013) via cluster analysis. These studies have limited capacity to understand the pathway of multimorbid conditions across the lifespan and possible shared biologic processes in the aetiology of specific diseases and the effects of multimorbidity on individual's intrinsic capacity and functional ability (Prados-Torres *and others*, 2014; Valderas *and others*, 2009; World Health Organization, 2015). Research on longitudinal multimorbidity data has been scarce or was limited by being exploratory in nature (Ashworth *and others*, 2019; Ruel *and others*, 2014; Vos *and others*, 2015).

In this paper, we take an innovative perspective on analysing longitudinal multimorbidiy data within a statistical framework of survival analysis, with an attempt to open a new way to advance the knowledge on the onset and the evolution pathway of multimorbidity. In survival analysis of longitudinal time-to-event data, there are a number of formidable challenges due to the heterogeneity in individual's risk of failure, the loss of the appealing cancellation property in the estimation process for the parameters in Cox regression models, and the presence of "informative censoring" due to a "terminal" event; see Ng *and others* (2019*b*) for an overview on these issues. Here, we develop a new joint frailty modelling approach via a generalised linear mixed model (GLMM) method to address the aforementioned methodological barriers for efficient estimation of model parameters. The advantages of frailty models are their capacity to account for heterogeneity in individual responses using (multivariate) random effects. Existing joint frailty modelling methods to handle informative censoring have been implemented by assuming a shared patient-specific frailty term under an integrated likelihood approach or a Bayesian setting; see, for example, Huang and Wolfe (2002); Liu *and others* (2016); Paulon *and others* (2020). In our approach, we consider a more general model that allows for two correlated random effects to jointly model the dependence between the hazard rates of recurrent events and the terminal event.

We provide an overview of the proposed joint frailty model and an application of the model to a real cancer registry data set on the multimorbidity of melanoma patients in Australia. We then document the performance of the joint frailty model via extensive simulation studies. These show that the proposed model performs well in a wide variety of contexts and it is superior to the natural competitor of a classical frailty model.

2. Methods

Suppose we follow up M independent patients from the study onset and observe the gap times of events experienced by each patient. The event of interest corresponds to a recurrent episode, such as tumour relapses or in this study multimorbidity of health conditions. Denote T_{jk}^R the gap times of the recurrent event and T_j^D the gap time from the last recurrent event to death, which are both subject to right censoring ($j = 1, \ldots, M;\ k = 1, 2, \ldots$). Here, death is considered as a terminal event, creating a mechanism of informative censoring where the recurrent and terminal events are correlated in contrast to a classical assumption of independent censoring in survival analysis (Huang and Wolfe, 2002; Liu *and others*, 2016; Tawiah *and others*, 2020*a*). That is, censoring due to death is informative for failure due to the recurrent event. On the other hand, the gap censoring time from the last event to the end of the study (also known as "administrative censoring"), denoted by C_j, is non-informative (Huang and Wolfe, 2002). Let $T_{jk} = \min(T_{jk}^R, T_j^D, C_j)$ and define the indicator variables for a recurrent event and death, respectively, $\delta_{jk}^R = 1$ if $T_{jk} = T_{jk}^R$, $\delta_j^D = 1$ if $T_{jk} = T_j^D$, and both to be 0 if censored (i.e. $T_{jk} = C_j$). The observed data on the jth patient is thus given by $O_j = \{(t_{jk}, \delta_{jk}^R, \delta_j^D, \boldsymbol{x}_j), j = 1, \ldots, M; k = 1, \ldots, n_j\}$, where $\boldsymbol{X}_j = (X_{j1}, \ldots, X_{jp})^T$ is a p-dimensional vector of risk variables and n_j denotes the number of observed gap times for the jth patient. The superscript T denotes vector transpose. Overall, there are $\sum_{j=1}^M n_j = N$ observations. In contrast to the use of a shared frailty term (Huang and Wolfe, 2002), we denote $\boldsymbol{u} = (u_1, \ldots, u_M)^T$ and $\boldsymbol{v} = (v_1, \ldots, v_M)^T$ be the random vectors of

u_j and v_j that represent the frailty for the jth patient to account for intra-subject correlation of multivariate recurrent event times and individual differences in mortality hazard rate for the death time, respectively. Assuming that $\boldsymbol{q} = (\boldsymbol{u}^T, \boldsymbol{v}^T)^T$ follows a multivariate normal distribution $N(\mathbf{0}, \boldsymbol{\Sigma})$, we consider the variance-covariance matrix as $\boldsymbol{\Sigma} = \Gamma \otimes I_M$, where

$$\Gamma = \begin{bmatrix} \theta_u^2 & \rho\theta_u\theta_v \\ \rho\theta_u\theta_v & \theta_v^2 \end{bmatrix} \tag{2.1}$$

and $\otimes$ denotes the Kronecker product of two matrices. In (2.1), θ_u^2 and θ_v^2 quantify the heterogeneity in the unobserved random (frailty) effects for the hazard rates of recurrent events and death, respectively, whereas a correlation parameter ρ is adopted to model the dependence between θ_u^2 and θ_v^2; see, for example, Tawiah *and others* (2020*a*).

Under the Cox proportional hazards (PH) model, the hazard functions for recurrent events and death are given by

$$\begin{aligned} h_R\left(t_{jk}^R; \boldsymbol{x}_j\right) &= h_{R0}\left(t_{jk}^R\right) \exp\left(\eta_{jk}\right), \\ h_D\left(t_j^D; \boldsymbol{x}_j\right) &= h_{D0}\left(t_j^D\right) \exp\left(\zeta_j\right), \end{aligned} \tag{2.2}$$

where $h_{R0}(t_{jk}^R)$ and $h_{D0}(t_j^D)$ are the baseline hazard functions, η_{jk} and ζ_j are the linear predictors for recurrent events and death, respectively, which relate to the risk covariates $\boldsymbol{x}_j$ as:

$$\eta_{jk} = \boldsymbol{x}_j^T\boldsymbol{\beta} + u_j \quad \text{and} \quad \zeta_j = \boldsymbol{x}_j^T\boldsymbol{\gamma} + v_j, \tag{2.3}$$

where $\boldsymbol{\beta}$ and $\boldsymbol{\gamma}$ are the vectors of fixed-effect regression coefficients for recurrent events and death, respectively. A positive value of coefficients in $\boldsymbol{\beta}$ or $\boldsymbol{\gamma}$ implies a higher risk of failure associated with the risk covariates.

2.1 *Joint modelling via GLMM*

We develop a GLMM method for the joint modelling of $h_R\left(t_{jk}^R; \boldsymbol{x}_j\right)$ and $h_D\left(t_j^D; \boldsymbol{x}_j\right)$ with random effects terms in η_{jk} and ζ_j; see (2.2) and (2.3). With this GLMM formulation, multivariate random

effects are added to the linear predictors and the corresponding partial log-likelihood of failure times with the random effects conditionally fixed can be constructed. Besides its capacity to assess and estimate the heterogeneity in individual risk of failure in recurrent events or death, another appealing aspect of the GLMM approach is to retain the cancellation property where the unknown baseline hazard functions are eliminated in the estimation process for the regression parameters, leading to more efficient estimation procedures relatively and that the baseline hazard functions can be unspecified (Ng *and others*, 2019*b*; Yau, 2001).

Denote $\boldsymbol{\Omega} = (\boldsymbol{\beta}^T, \boldsymbol{\gamma}^T, \boldsymbol{u}^T, \boldsymbol{v}^T)^T$. The GLMM method starts with developing best linear unbiased prediction (BLUP) estimators for $\boldsymbol{\Omega}$ that maximise the sum of two components:

$$\begin{aligned} l_1 &= \text{ Joint partial log-likelihood of failure times taking } \boldsymbol{u} \text{ and } \boldsymbol{v} \text{ fixed,} \\ l_2 &= -\frac{1}{2}\left\{M\log(2\pi|\boldsymbol{\Sigma}|) + (\boldsymbol{u}^T, \boldsymbol{v}^T)\boldsymbol{\Sigma}^{-1}(\boldsymbol{u}^T, \boldsymbol{v}^T)^T\right\}, \end{aligned} \tag{2.4}$$

where l_2 is the logarithm of the joint probability density function of random effects $\boldsymbol{u}$ and $\boldsymbol{v}$.

To write down the partial log-likelihood l_1, the recurrent event gap/censoring times and the death/censoring times are arranged in increasing order, with their corresponding linear predictors and indicator variables representing failure or censoring. The respective distinct reordered uncensored times are denoted by $t_{i1}, \ldots, t_{iK_i}$ for $i = R$ (recurrent events) and $i = D$ (death). Assuming a step function with discontinuities at each observed failure time for the baseline hazard functions $h_{i0}(t_i)$ for recurrent events ($i = R$) or death ($i = D$), it can be shown from Breslow (1974) that the joint partial log-likelihood for the Cox PH model, conditional on fixed random effects, is given by:

$$l_1 = \sum_{r=1}^{K_R}\left\{\eta_r - m_r^R \log \sum_{l\in R(t_{Rr})} \exp(\eta_l)\right\} + \sum_{r=1}^{K_D}\left\{\zeta_r - m_r^D \log \sum_{l\in R(t_{Dr})} \exp(\zeta_l)\right\}, \tag{2.5}$$

where m_r^i is the number of uncensored failures at t_{ir} ($i = R$ or $i = D$), η_r and ζ_r represent the sum of linear predictors over the m_r^R and m_r^D tied observed failures, respectively, and $R(t_{Rr})$ and $R(t_{Dr})$ are the risk sets at time t_{Rr} and t_{Dr} corresponding to the gap times of the recurrent

events and the death times, respectively. Based on the BLUP estimates, the approximate residual maximum likelihood (REML) estimate of the variance component parameters in $\boldsymbol{\Sigma}$, denoted as $\boldsymbol{\Phi} = (\theta_u^2, \theta_v^2, \rho)^T$, is then obtained by solving the equation of the first-order derivative of the REML log likelihood with respect to $\boldsymbol{\Phi}$ (Yau, 2001). The asymptotic variances of the estimates in $\boldsymbol{\beta}$, $\boldsymbol{\gamma}$, and $\boldsymbol{\Phi}$ are then obtained via the second derivative of $l = l_1 + l_2$ with respect to the conformal partition of $\boldsymbol{\beta}|\boldsymbol{\gamma}|\boldsymbol{u}|\boldsymbol{v}$, as outlined in Section S1 of supplementary material available at *Biostatistics* Online.

2.2 *Algorithm*

The Newton-Raphson iterative procedure is adopted to update the BLUP estimates by finding the solution that maximises (2.4). Let $\boldsymbol{X}_1, \boldsymbol{X}_2, \boldsymbol{Z}_1$ and $\boldsymbol{Z}_2$ denote the design matrices of $\boldsymbol{\beta}, \boldsymbol{\gamma}, \boldsymbol{u}$ and $\boldsymbol{v}$, respectively, and $\boldsymbol{G}^{-1}$ denote the inverse of the information matrix corresponding to l. In the kth iteration, we have:

$$\begin{bmatrix} \boldsymbol{\beta}^{(k)} \\ \boldsymbol{\gamma}^{(k)} \\ \boldsymbol{u}^{(k)} \\ \boldsymbol{v}^{(k)} \end{bmatrix} = \begin{bmatrix} \boldsymbol{\beta}^{(k-1)} \\ \boldsymbol{\gamma}^{(k-1)} \\ \boldsymbol{u}^{(k-1)} \\ \boldsymbol{v}^{(k-1)} \end{bmatrix} + \boldsymbol{G}^{-1} \begin{bmatrix} \partial l/\partial \boldsymbol{\beta} \\ \partial l/\partial \boldsymbol{\gamma} \\ \partial l/\partial \boldsymbol{u} \\ \partial l/\partial \boldsymbol{v} \end{bmatrix}, \tag{2.6}$$

where

$$\frac{\partial l}{\partial \boldsymbol{\beta}} = \boldsymbol{X}_1^T \frac{\partial l_1}{\partial \eta}; \quad \frac{\partial l}{\partial \boldsymbol{\gamma}} = \boldsymbol{X}_2^T \frac{\partial l_1}{\partial \zeta};$$

$$\frac{\partial l}{\partial \boldsymbol{u}} = \boldsymbol{Z}_1^T \frac{\partial l_1}{\partial \eta} - \frac{\boldsymbol{u}\theta_v^2 - \boldsymbol{v}\rho\theta_u\theta_v}{\theta_u^2\theta_v^2(1-\rho^2)}; \quad \frac{\partial l}{\partial \boldsymbol{v}} = \boldsymbol{Z}_2^T \frac{\partial l_1}{\partial \zeta} - \frac{\boldsymbol{v}\theta_u^2 - \boldsymbol{u}\rho\theta_u\theta_v}{\theta_u^2\theta_v^2(1-\rho^2)};$$

see Section S1 of supplementary material available at *Biostatistics* Online for the block matrices of $\boldsymbol{G}^{-1}$ and the derivation of $\partial l_1/\partial\eta$ and $\partial l_1/\partial\zeta$.

By solving the equation of the first order derivative of the REML log likelihood with respect to $\boldsymbol{\Phi}$, it follows that an update of the approximate REML estimators of $\boldsymbol{\Phi}$ is given by:

$$\theta_u^2 = \frac{1}{M}\Im_1, \quad \rho = \frac{1}{\sqrt{\Im_1\Im_3}}\Im_2, \quad \text{and} \quad \theta_v^2 = \frac{1}{M}\Im_3, \tag{2.7}$$

where

$$\Im_1 = \text{tr}\left\{K_1\left(\boldsymbol{B}_{q,q} + \boldsymbol{q}\boldsymbol{q}^T\right)\right\},$$

$$\Im_2 = \text{tr}\left\{K_2\left(\boldsymbol{B}_{q,q} + \boldsymbol{q}\boldsymbol{q}^T\right)\right\}/2,$$

$$\Im_3 = \text{tr}\left\{K_3\left(\boldsymbol{B}_{q,q} + \boldsymbol{q}\boldsymbol{q}^T\right)\right\}$$

are calculated based on the current estimates of $\boldsymbol{\Omega}$. Here, tr denotes the trace of a matrix, $\boldsymbol{B}_{q,q}$ is the block matrix of $\boldsymbol{G}^{-1}$ corresponding to the random effects $\boldsymbol{q}$, and the block matrices K_1, K_2 and K_3 are defined as:

$$K_1 = \begin{bmatrix} I_M & 0 \\ 0 & 0 \end{bmatrix}, \quad K_2 = \begin{bmatrix} 0 & I_M \\ I_M & 0 \end{bmatrix}, \quad \text{and} \quad K_3 = \begin{bmatrix} 0 & 0 \\ 0 & I_M \end{bmatrix};$$

see Section S1 of supplementary material available at *Biostatistics* Online for the formulation of $\boldsymbol{B}_{q,q}$.

The following summarises the computational procedure for the proposed joint modelling of recurrent and death times within the GLMM framework:

1. Set the initial values of $\boldsymbol{\Omega}^{(0)}$ (corresponding to $\boldsymbol{\beta}^{(0)}$, $\boldsymbol{\gamma}^{(0)}$, $\boldsymbol{u}^{(0)}$, and $\boldsymbol{v}^{(0)}$) to zero and the initial values of $\boldsymbol{\Phi}^{(0)}$ (corresponding to $\theta_u^{2(0)}$, $\theta_v^{2(0)}$, and $\rho^{(0)}$) to relatively small values.

2. Given the current estimates of $\boldsymbol{\Omega}$ and $\boldsymbol{\Phi}$, update the estimates of $\boldsymbol{\Omega}$ using (2.6) until convergence.

3. Update the variance component parameters in $\boldsymbol{\Phi}$ using (2.7).

4. Repeat Steps 2 and 3 until convergence.

5. Calculate the standard errors of estimates in $\boldsymbol{\Omega}$ using the block matrices $\boldsymbol{B}_{\beta,\beta}$ and $\boldsymbol{B}_{\gamma,\gamma}$ in Equation (S1.1) of supplementary material available at *Biostatistics* Online, respectively.

6. Calculate the standard errors of estimates in $\boldsymbol{\Phi}$ using Equation (S1.5) of supplementary material available at *Biostatistics* Online, corresponding to the inversion of the REML information matrix.

2.3 *Estimation of baseline survival function and mean residual life function*

Given $\hat{\boldsymbol{\Omega}}$, the baseline survival functions corresponding to the baseline hazard functions for recurrent events and death, respectively, $h_{R0}(t^R_{jk})$ and $h_{D0}(t^D_j)$ can be estimated using the Breslow-type estimator (Breslow, 1974). That is,

$$\hat{S}_{R0}(t_{Rr}) = \exp\left\{-\sum_{r=1}^{K_R}\left(\frac{m^R_r}{\sum_{l\in R(t_{Rr})}\exp(\eta_l)}\right)\right\},$$
$$\hat{S}_{D0}(t_{Dr}) = \exp\left\{-\sum_{r=1}^{K_D}\left(\frac{m^D_r}{\sum_{l\in R(t_{Dr})}\exp(\zeta_l)}\right)\right\} \tag{2.8}$$

for $r = (1, \ldots, K_i)$, where $i = R$ (recurrent events) or $i = D$ (death). With the Cox PH model (2.2), the overall estimated survival function at time t conditioned on risk variables $\boldsymbol{X}$ is given by

$$\hat{S}(t;\boldsymbol{X}) = \hat{S}_{R0}(t)^{\exp(\boldsymbol{X}^T\hat{\boldsymbol{\beta}})}\hat{S}_{D0}(t)^{\exp(\boldsymbol{X}^T\hat{\boldsymbol{\gamma}})}, \tag{2.9}$$

which summarises failure risk in terms of the probability of survival (free from recurrent event or death) at any time point t.

A popular alternative to the survival function (2.9) is the mean residual life (MRL) function which summarises failure risk in terms of the remaining life expectancy (i.e. in a unit of time rather than a probability). The concept of the MRL has been widely used in operational research, reliability and statistics (Si *and others*, 2011). For a non-negative failure time T with finite expectation, the MRL function at time t given $\boldsymbol{X}$ is defined as

$$m(t;\boldsymbol{X}) = E(T-t|T>t;\boldsymbol{X}) = \frac{\int_t^\infty S(s;\boldsymbol{X})ds}{S(t;\boldsymbol{X})}, \tag{2.10}$$

providing the information on the remaining expected lifetime given risk variables $\boldsymbol{X}$ and survival up to time t (Alvarez-Iglesias *and others*, 2015; Sun and Zhang, 2009). In this study, the MRL function is estimated by replacing $S(t;\boldsymbol{X})$ in (2.10) by the estimated survival function $\hat{S}(t;\boldsymbol{X})$ from (2.9) via the PH assumption. The proportionality assumption in the hazard functions is a widely used and well established approach in survival analysis, which is in contrast to the

proportional MRL assumption (Chen *and others*, 2005; Huang *and others*, 2019; Sun and Zhang, 2009). In applications where the estimation of the tail of $S_{i0}(t)$ is required ($i = R$ or $i = D$), for example when the largest observed gap time is censored, the exponential-tail (ETAIL) completion method can be adopted to provide an estimate for $S_{i0}(t)$; see Peng (2003); Tawiah *and others* (2020*b*). That is,

$$\hat{S}_{i0}(t) = \exp(-\hat{\lambda}_i t) \qquad (t > t_{hi}), \tag{2.11}$$

where t_{hi} is the largest uncensored gap time ($i = R$ or $i = D$) and $\hat{\lambda} = -\log\{\hat{S}_{i0}(t_{hi})\}/t_{hi}$.

3. Results

3.1 *A real example*

The Queensland melanoma cancer registry data identify melanoma patients diagnosed and treated at Queensland hospitals in Australia in 2005 with follow-up until 2015. In this study, the Queensland melanoma cancer registry data were retrieved for melanoma patients aged > 50 years, diagnosed and treated in Queensland in 2005. The occurrence of secondary primary cancer other than melanoma amongst this population during the follow-up period up to December 2015 was identified using International Classification of Diseases for Oncology (ICD-O) codes. Demographic and clinical information included age at diagnosis (relative to the age of 50 years), gender, country of birth (Overseas versus Australian-born), remoteness of residence at diagnosis (Outer regional/Remote/Very remote versus Major city/Inner regional), melanoma site (skin of trunk or skin of upper/lower limbs versus head/neck), lesion thickness ($>$ 1mm versus $\leqslant$ 1mm), and ulceration (presence versus absence). The data set consists of 1,624 observations from 1,399 patients. There are 491 deaths, corresponding to a censoring proportion of 64.9% for δ_j^D. The results of applying the proposed joint frailty model are presented in Table 1, along with those using a standard frailty model via the GLMM without the assumption of informative censoring for comparison (the coxme package in R developed by Therneau (2018) produced the same conclusion

for the standard frailty model).

With the joint frailty model, it can be seen from Table 1 that older, male patients are associated with an increased risk for multimorbidity of a secondary cancer (HR=1.038 per year older, 95% CI = 1.022 to 1.054, $p < 0.001$; HR = 1.964 for male, 95% CI = 1.367 to 2.822, $p < 0.001$) and death (HR=1.113 per year older, 95% CI = 1.098 to 1.128, $p < 0.001$; HR = 2.022 for male, 95% CI = 1.522 to 2.686, $p < 0.001$). Patients with ulceration also have increased risks for multimorbidity (HR=2.683, 95% CI = 1.644 to 4.380, $p < 0.001$) as well as death (HR = 2.487, 95% CI = 1.748 to 3.539, $p < 0.001$). Compared to patients living in major city or inner regional areas, those patients who are living in outer regional, remote, or very remote areas have a lower hazard risk for multimorbidity (HR = 0.613, 95% CI = 0.381 to 0.984, $p = 0.043$) but a non-significant effect for risk of death. On the other hand, patients with lesion thickness > 1mm have a negligible effect in risk of multimorbidity but a higher risk for death (HR = 1.799, 95% CI = 1.327 to 2.437, $p < 0.001$). Furthermore, patients with melanoma at skin of upper or lower limbs have a reduced risk of death (HR = 0.643, 95% CI = 0.465 to 0.891, $p = 0.008$) compared to those with melanoma at skin of head or neck. The estimate of the frailty variance parameters θ_u^2, θ_v^2, and ρ are large and significant, indicating that there are meaningful heterogeneity in individual's risk of failure and positive dependence between the hazard rate of multimorbidity and death. The latter implies that the incidence of comorbid cancer is associated with poor survival outcomes with an increased risk of death.

While the results from the standard frailty model given in Table 1 are comparable with those from the proposed joint frailty model, some slight differences can be observed. In particular, the estimate of the frailty variance parameter θ_u^2 is considerably smaller (about one third of that in the joint frailty model). In practice, a major drawback of the standard frailty model is the lack of information regarding death as a terminal event and its adjustment in the survival analysis; see also further comparisons between the joint frailty model and the standard frailty model via

simulations in the next subsection.

The estimated survival curves with respect to multimorbidity and death by age for male and female patients living in major city or inner regional areas with melanoma site at head or neck, leison thickness > 1mm, and ulceration are displayed in Figures 1a and 1b. The corresponding MRL functions are given in Figures 2a and 2b. It can be seen that the probability of survival (event free) is significantly higher for female patients and those diagnosed at a younger age. For example, around 50% of male patients aged 50 years at diagnosis will survive 10 years of event free for multimorbidity of a secondary cancer or death, whereas 70% of female patients aged 50 years will have the same survival period. The MRL functions shown in Figure 2 indicate slightly increasing hazard over time (constant hazard is observed after 8 years post-diagnosis for younger patients). On average, male patients diagnosed at the age of 50 years have roughly 13-year event-free period initially; those patients survived past 5 years post-diagnosis will have about 10.5 years event-free time. Again, there is evidence of significant age and gender differences. For example, it is estimated that male patients diagnosed at the age of 60 years have multimorbidity of a secondary cancer or death approximately 6 years earlier compared with male patients diagnosed at the age of 50 years. Comparing patients diagnosed at the age of 50 years, females are event free for approximately 11.5 years more than males (see Figures 2a and 2b).

3.2 *Simulation studies*

Based on a cancer registry data structure, we generate $\boldsymbol{X}_j$, T_{jk}^R, T_j^D, and S_j for $M = 500$ patients as follows: (a) Two-dimensional ($p = 2$) vector of $\boldsymbol{X}_j$: a binary covariate variable X_{j1} is generated from Bernoulli distribution with a 0.5 probability, whereas a continuous covariate variable X_{j2} is generated from a standard normal distribution N(0,1); (b) Correlated gap times to recurrent events and death: multivariate random vector $\boldsymbol{q}$ is generated from the multivariate normal distribution $N(\mathbf{0}, \Gamma \otimes I_M)$ given Γ in (2.1) and parameters θ_u^2, θ_v^2 and ρ, then the gap times T_{jk}^R and T_j^D

are generated using the cumulative hazard inversion method from the joint frailty model (2.2) given parameters $\boldsymbol{\beta}$ and $\boldsymbol{\gamma}$, where the baseline hazards are taken to be Weibull distributions with scale parameter λ_i and shape parameter τ_i for $i = R$ or $i = D$; (c) Administrative follow-up time S_j is generated from a uniform distribution $U(a, b)$ representing a cancer registry with follow-up of at least a days.

For each patient $j = (1, \ldots, M)$, the observed failure time t_{jk} is obtained by $t_{jk} = \min(t_{jk}^R, t_j^D, C_j)$ repeatedly until $\sum_k t_{jk} \geqslant S_j$. The last event is either death ($t_{jk} = t_j^D$) or censored ($t_{jk} = C_j$). The indicator variables δ_{jk}^R and δ_j^D are obtained according to the type of the event for $j = 1, \ldots, M;\ k = 1, \ldots, n_j$. We compare the proposed joint frailty model with informative censoring to the classical frailty model under eight sets of scenario in a wide variety of contexts. Assessment is based on 500 replicated simulations for each set. Table 2 presents the comparison for the first six sets, in terms of the average bias, the average of the standard error estimates (SEE), the sample standard error of the estimates over 500 replications (SE), and the coverage probability (CP) of 95% confidence interval based on the normal approximation. Two additional simulated data sets, presented in Table S1 of supplementary material available at *Biostatistics* Online, assess the performance under a different setting of covariate effects and examine the robustness of the model to mis-specification of the normality assumption of the random effects.

Set 1 in Table 2 is the base model. We consider Weibull distributions with a low start but increasing hazard ($\lambda_R = 3 \times 10^{-6}$; $\lambda_D = 2 \times 10^{-6}$; $\tau_R = 1.3$; $\tau_D = 1.5$) and moderate variance component parameters ($\theta_u = \theta_v = \rho = 0.8$). Covariate effects are specified in $\boldsymbol{\beta}$ and $\boldsymbol{\gamma}$ such that the binary covariate variable X_{j1} reduces failure risk of multimorbidity and death, whereas the continuous covariate variable X_{j2} increases both failure risks. We take $a = 1825$ and $b = 2200$ for an administrative follow-up period of at least 5 years. The averaged censoring proportion of 500 replicated simulations for δ_j^D is 83.7% .

In Sets 2 and 3, we assess the performance of the models under the scenarios of increased

variance component parameters ($\theta_u = \theta_v = 1.5$ and $\rho = 0.9$; $\theta_u = \theta_v = 2$ and $\rho = 0.95$, respectively; the latter corresponds to a setting close to that of the real melanoma data set in Table 1). We also raise the hazard risks ($\tau_R = 1.5$ and $\tau_D = 1.7$; $\tau_R = 1.6$ and $\tau_D = 1.8$, respectively). The corresponding averaged censoring proportions for δ_j^D in Sets 2 and 3 are 57.3% and 43.8%, respectively.

In Set 4, we study the situation where the dependence between multimorbidity and death is small ($\rho = 0.2$) while keeping all other parameters the same as those in the base model in Set 1. The corresponding averaged censoring proportion for δ_j^D in Set 4 is 83.6%. Next, we consider a longer follow-up period of at least 10 years by taking $a = 3650$ and $b = 4000$ in Set 5 and a large sample size ($M = 1000$) in Set 6 (the averaged censoring proportion for δ_j^D are 68.5% and 83.8%, respectively). All other parameters are set as in the base model.

In Set 7 (Table S1 of supplementary material available at *Biostatistics* Online), we assess the performance under a different setting of covariate effects (here, both X_{j1} and X_{j2} increase the risk of multimorbidity, whereas X_{j1} increases but X_{j2} reduces the risk of death). Finally in Set 8, we examine the robustness of the model to mis-specification of the normality assumption of the random effects by generating $\boldsymbol{q}$ from mixtures of two normal distributions. The corresponding averaged censoring proportions for δ_j^D in Sets 7 and 8 are 71.3% and 84.0%, respectively.

From Table 2 and Table S1 of supplementary material available at *Biostatistics* Online, no appreciable bias is observed in all simulation settings, confirming the applicability of the proposed joint frailty model in a wide variety of contexts. In general, there is good agreement between SEE and SE for all the fixed-effect parameters, indicating that the standard errors of these parameters are well estimated. The SEE and SE are also comparable for the variance components, except θ_u for multimorbidity when the variance component parameters are small ($\leqslant 0.8$ in all sets except Sets 2 and 4). This is also reflected in the CP, which is lower than the nominal level. This finding implies that the standard error of θ_u^2 may be underestimated in some situations and thus caution

should be exercised in interpreting the significance level to this variance component parameter; see Tawiah *and others* (2020*a*,*b*) for discussion on formal tests of heterogeneity when prediction of subject-specific frailties is relevant. As expected, settings with a longer follow-up or larger sample size in Sets 5 and 6 lead to improved results (e.g., lower SE or better CP). Comparatively, the estimates obtained from the standard frailty model have generally a larger bias. In particular, when the variance component parameters are large (Sets 2 and 3), the estimates of the fixed-effect and variance component parameters are heavily biased. In all settings, the standard errors of θ_u^2 are overestimated.

4. Discussion

Multimorbidity is increasingly recognised as an important issue in health sciences, imposing serious challenges on the world's healthcare systems. Modern study designs and data-linkage technologies have enabled collection of longitudinal data that can advance our knowledge on the evolution of multimorbidity, which is valuable for developing interventions and care management strategies to better help the large number of individuals with multiple conditions. What is missing is an efficient modelling technique to overcome the methodological barriers in time-to-event data analyses, due to heterogeneous failure risk and the presence of a terminal event. In this paper, we have developed a new joint frailty modelling framework within the GLMM for efficient estimation of model parameters in survival analysis of recurrent time-to-event data. This is timely given the heavy investments worldwide in conducting large-scale studies associated with multimorbidity.

Our approach retains the cancellation of baseline hazard property, which makes the estimation procedures relatively efficient. It also yields a more general model through the use of multivariate random effects to model jointly the dependence between the hazard rates of recurrent events and a terminal event. More importantly, the proposed joint frailty model provides clinically important information on event-free survival and residual life as well as prediction of patient-

specific frailties for both recurrent and terminal events, beyond those that can be observed from existing frailty models. The applicability of the proposed method to advance our knowledge on the evolution of multimorbidity is illustrated using a real cancer registry data of melanoma patients in Australia, where multimorbidity is referred to as the occurrence of secondary primary cancer other than melanoma. We show how the failure risk of multimorbidity and death can be summarised using the estimated survival and MRL functions. The performance of the joint frailty model is demonstrated via simulation studies, which show its superiority over the standard frailty model and its robustness in a wide variety of contexts and to the violation of normality assumption of random effects.

In some circumstances in the survival analysis of recurrent event data, there may exist a subgroup of patients who have recovered (or cured) and thus will not experience any failure event. In these situations, a joint frailty mixture cure model can be adopted to explain the patient-specific frailties that affect the cure proportion in the incidence component via logistic modelling (Tawiah *and others*, 2020*b*). Justification of the use of cure models requires the evidence of the existence of so-called "long-term survivors", which is characterised by the survival curves being levelled at non-zero probabilities (Tawiah *and others*, 2020*a*). The survival curves displayed in Figure 1 do not suggest the necessity of a cure model for analysing the melanoma cancer registry data.

The proposed method can be readily applicable to solve health problems in the general context of multimorbidity. In this context, time to multimorbidity corresponds to the occurrence of comorbid chronic diseases within an individual. But the proposed joint frailty model does not distinguish the types of chronic diseases in each event. While this issue may be handled by incorporating the disease type in the modelling of recurrent events (see Beesley and Taylor (2019)), the complexity of the joint frailty model so formed will be increased such that efficient estimation of model parameters via the GLMM may be hard to retain. Alternatively, multi-state survival

models may be adopted to account for competing events at each transition between disease states; see, for example, Crowther and Lambert (2017); Williams *and others* (2020). This approach emphasises on the modelling of transition probabilities using Markov or semi-Markov models and provides a different kind of information regarding covariate effects for each specific transition between two disease states. The integration of this approach into the joint frailty model, along with other model extensions such as the accelerated failure time (AFT) or "interval censoring" assumptions, will be pursued in future research.

5. Software

Software in the form of R code, together with a de-identified sample input data set and complete documentation for the proposed joint frailty modelling is available on request from the corresponding author (s.ng@griffith.edu.au).

6. Supplementary Material

Supplementary material is available online at `http://biostatistics.oxfordjournals.org`.

Acknowledgments

This work was partly supported by the Australian Research Council (Grant Number: DP170100907).

Conflict of Interest: None declared.

References

Academy of Medical Science. (2018). *Multimorbidity: A Priority for Global Health Research*. London: The Academy of Medical Sciences.

Alvarez-Iglesias, A., Newell, J., Scarrott, C. and Hinde, J. (2015). Summarising censored survival data using the mean residual life function. *Statistics in Medicine* **34**, 1965–1976.

Ashworth, M., Durbaba, S., Whitney, D., Crompton, J., Wright, M. and Dodhia, H. (2019). Journey to multimorbidity: longitudinal analysis exploring cardiovascular risk factors and sociodemographic determinants in an urban setting. *BMJ Open* **9**, e031649.

Beesley, L. J. and Taylor, J. M. G. (2019). EM algorithms for fitting multistate cure models. *Biostatistics* **20**, 416–432.

Breslow, N. E. (1974). Covariance analysis of censored survival data. *Biometrics* **30**, 89–99.

Chen, Y. Q., Jewell, N. P., Lei, X. and Cheng, S. C. (2005). Semiparametric estimation of proportional mean residual life model in presence of censoring. *Biometrics* **61**, 170–178.

Crowther, M. J. and Lambert, P. C. (2017). Parametric multistate survival models: Flexible modelling allowing transition-specific distributions with application to estimating clinically useful measures of effect differences. *Statistics in Medicine* **36**, 4719–4742.

Di Angelantonio, E., Kaptoge, S., Wormser, D. and Willeit, P. (2015). Association of cardiometabolic multimorbidity with mortality. *Journal of American Medical Association* **314**, 52–60.

Huang, R., Xiang, L. and Ha, I. D. (2019). Frailty proportional mean residual life regression

for clustered survival data: A hierarchical quasi-likelihood method. *Statistics in Medicine* **38**, 4854–4870.

Huang, X. and Wolfe, R. A. (2002). A frailty model for informative censoring. *Biometrics* **58**, 510–520.

Lancet editorial. (2018). Making more of multimorbidity: an emerging priority. *Lancet* **391**, 1637.

Liu, L., Huang, X., Yaroshinsky, A. and Cormier, J. N. (2016). Joint frailty models for zero-inflated recurrent events in the presence of a terminal event. *Biometrics* **72**, 204–214.

Marengoni, A., Rizzuto, D., Wang, H. X., Winblad, B. and Fratiglioni, L. (2009). Patterns of chronic multimorbidity in the elderly population. *Journal of American Geriatrics Society* **57**, 225–230.

Ng, S. K. (2015). A two-way clustering framework to identify disparities in multimorbidity patterns of mental and physical health conditions among Australians. *Statistics in Medicine* **34**, 3444–3460.

Ng, S. K., Holden, L. and Sun, J. (2012). Identifying comorbidity patterns of health conditions via cluster analysis of pairwise concordance statistics. *Statistics in Medicine* **31**, 3393–3405.

Ng, S. K., Tawiah, R. and McLachlan, G. J. (2019*a*). Unsupervised pattern recognition of mixed data structures with numerical and categorical features using a mixture regression modelling framework. *Pattern Recognition* **88**, 261–271.

Ng, S. K., Tawiah, R., Sawyer, M. and Scuffham, P. (2018). Patterns of multimorbid health conditions: A systematic review of analytical methods and comparison analysis. *International Journal of Epidemiology* **47**, 1687–1704.

Ng, S. K., Xiang, L. and Yau, K. W. W. (2019*b*). *Mixture Modelling for Medical and Health Sciences*. Boca Raton, FL: Chapman & Hall/CRC, Chapters 4 and 6.

Paulon, G., De Iorio, M., Guglielmi, A. and Ieva, F. (2020). Joint modeling of recurrent events and survival: a Bayesian non-parametric approach. *Biostatistics* **21**, 1–14.

Pearson-Stuttard, J., Ezzati, M. and Gregg, E. W. (2019). Multimorbidity – a defining challenge for health systems. *Lancet Public Health* **4**, e599–e600.

Peng, Y. (2003). Estimating baseline distribution in proportional hazards cure models. *Computational Statistics & Data Analysis* **42**, 187–201.

Prados-Torres, A., Calderón-Larrañaga, A., Hancco-Saavedra, J., Poblador-Plou, B. and van Den Akker, M. (2014). Multimorbidity patterns: a systematic review. *Journal of Clinical Epidemiology* **67**, 254–266.

Richardson, S., Hirsch, J. S., Narasimhan, M., Crawford, J. M., McGinn, T. and Davidson, K. W. (2020). Presenting characteristics, comorbidities, and outcomes among 5700 patients hospitalized with COVID-19 in the New York City area. *Journal of American Medical Association* **323**, 2052–2059.

Ruel, G., Lévesque, J.-F., Stocks, N., Sirois, C., Kroger, E., Adams, R. J., Doucet, M. and Taylor, A. W. (2014). Understanding the evolution of multimorbidity: Evidences from the North West Adelaide Health Longitudinal Study (NWAHS). *PLOS One* **9**, e96291.

Si, X.-S., Wang, W., Hu, C.-H. and Zhou, D.-H. (2011). Remaining useful life estimation – a review on the statistical data driven approaches. *European Journal of Operational Research* **213**, 1–14.

Sun, L. and Zhang, Z. (2009). A class of transformed mean residual life models with censored survival data. *Journal of American Statistical Association* **104**, 803–815.

Tawiah, R., McLachlan, G. J. and Ng, S. K. (2020*a*). A bivariate joint frailty model with mixture framework for survival analysis of recurrent events with dependent censoring and cure fraction. *Biometrics* **76**, 753–766.

Tawiah, R., McLachlan, G. J. and Ng, S. K. (2020*b*). Mixture cure models with time-varying and multilevel frailties for recurrent event data. *Statistical Methods in Medical Research* **29**, 1368–1385.

Therneau, T. (2018). Mixed Effects Cox Models. Avaliable at https://cran.r-project.org/web/packages/coxme/vignettes/coxme.pdf, Assessed on April 9, 2019.

Valderas, J. M., Starfield, B., Sibbald, B., Salisbury, C. and Roland, M. (2009). Defining comorbidity: implications for understanding health and health services. *Annals of Family Medicine* **7**, 357–363.

van den Akker, M., Buntinx, F. and Knotterus, J. (1996). Comorbidity or multimorbidity: what's in a name? A review of literature. *European Journal of General Practice* **2**, 65–70.

Vanfleteren, L. E., Spruit, M. A., Groenen, M., Gaffron, S., van Empel, V. P., Bruijnzeel, P. L., Rutten, E. P., Roodt, J. O., Wouters, E. F. and Franssen, F. M. (2013). Clusters of comorbidities based on validated objective measurements and systemic inflammation in patients with chronic obstructive pulmonary disease. *American Journal of Respiratory and Critical Care Medicine* **187**, 728–735.

Vos, R., van den Akker, M., Boesten, J., Robertson, C. and Metsemakers, J. (2015). Trajectories of multimorbidity: exploring patterns of multimorbidity in patients with more than ten chronic health problems in life course. *BMC Family Practice* **16**, 2.

Williams, J. P., Storlie, C. B., Therneau, T. M., Jack Jr, C. R. and Hannig, J.

(2020). A Bayesian approach to multistate hidden Markov models: Application to dementia progression. *Journal of American Statistical Association* **115**, 16–31.

World Health Organization. (2015). *World Report on Ageing and Health*. World Health Organization.

Yau, K. W. W. (2001). Multilevel models for survival analysis with random effects. *Biometrics* **57**, 96–102.

[*Received August 1, 2010; revised October 1, 2010; accepted for publication November 1, 2010*]

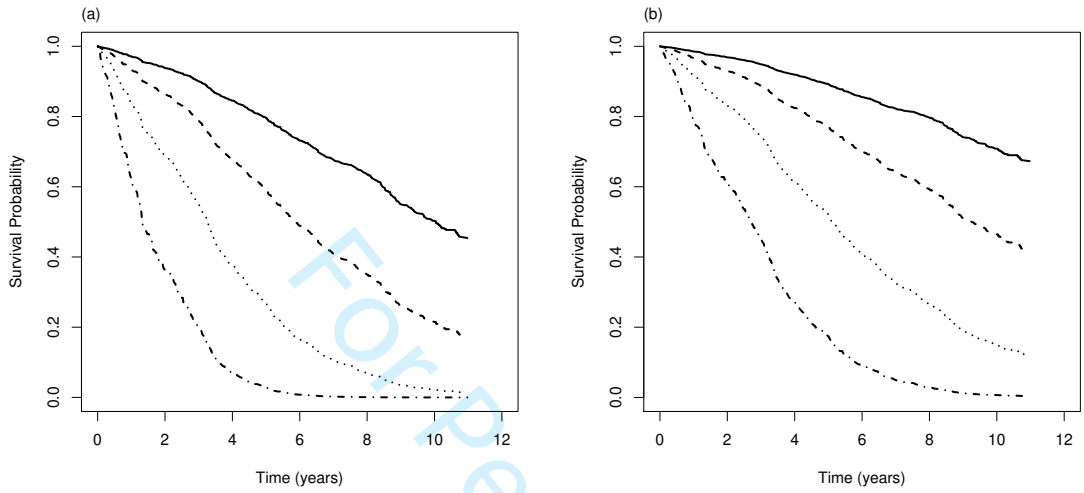

Fig. 1. Estimated survival curves by age for (a) male patients and (b) female patients (Age at diagnosis: 50 years (Solid line); 60 years (Dashed line); 70 years (Dotted line); 80 years (Dashed-dotted line)).

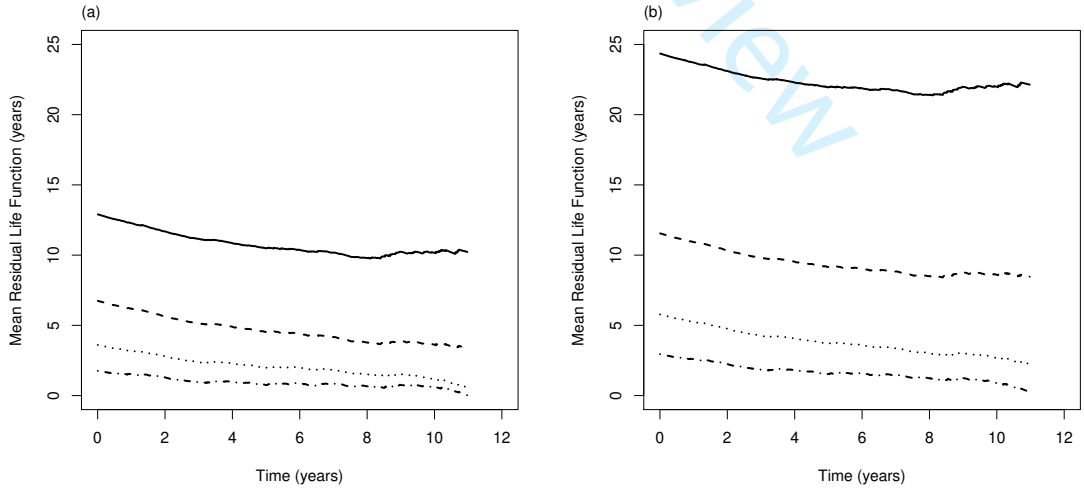

Fig. 2. Estimated mean residual life functions by age for (a) male patients and (b) female patients (Age at diagnosis: 50 years (Solid line); 60 years (Dashed line); 70 years (Dotted line); 80 years (Dashed-dotted line)).

Table 1. *Results of fitting the proposed joint frailty model and a standard frailty model to the melanoma cancer registry data*

	Parameter	Joint frailty model Hazard ratio (95% CI)	Frailty model Hazard ratio (95% CI)
Multimorbidity	Age	1.038 (1.022, 1.054)	1.026 (1.012, 1.041)
	Male	1.964 (1.367, 2.822)	1.905 (1.376, 2.637)
	Remoteness	0.613 (0.381, 0.984)	0.622 (0.406, 0.952)
	Melanoma site		
	Trunk	0.900 (0.560, 1.447)	0.896 (0.590, 1.360)
	Upper/lower limbs	1.012 (0.647, 1.582)	1.090 (0.736, 1.613)
	Head/Neck	Reference	Reference
	Thickness > 1mm	0.925 (0.615, 1.391)	0.819 (0.569, 1.179)
	Ulceration	2.683 (1.644, 4.380)	2.022 (1.311, 3.118)
Death	Age	1.113 (1.098, 1.128)	n.a.
	Male	2.022 (1.522, 2.686)	n.a.
	Remoteness	0.819 (0.580, 1.156)	n.a.
	Melanoma site		
	Trunk	0.753 (0.531, 1.067)	n.a.
	Upper/lower limbs	0.643 (0.465, 0.891)	n.a.
	Head/Neck	Reference	n.a.
	Thickness > 1mm	1.799 (1.327, 2.437)	n.a.
	Ulceration	2.487 (1.748, 3.539)	n.a.
Patient frailty	θ_u^2	1.978 (1.735, 2.221)	0.687 (0.224, 1.150)
	θ_v^2	1.968 (1.725, 2.211)	n.a.
	ρ	0.964 (0.958, 0.970)	n.a.

Table 2. *Results of simulated data (Sets 1 to 6)*

	Parameter (True value)	Joint frailty model				Frailty model			
		Bias	SEE	SE	CP	Bias	SEE	SE	CP
Set 1	β_1 (−0.6)	0.029	0.37	0.36	0.96	0.060	0.36	0.36	0.95
	β_2 (0.8)	-0.034	0.19	0.19	0.93	-0.053	0.18	0.19	0.92
	γ_1 (−0.8)	0.012	0.25	0.24	0.97		n.a.		
	γ_2 (0.5)	0.019	0.13	0.12	0.96		n.a.		
	θ_u (0.8)	0.048	0.06	0.17	0.85	-0.146	0.73	0.27	1.00
	θ_v (0.8)	0.030	0.06	0.11	0.88		n.a.		
	ρ (0.8)	0.008	0.02	0.03	0.88		n.a.		
Set 2	β_1 (−0.6)	0.067	0.24	0.23	0.95	0.190	0.22	0.23	0.82
	β_2 (0.8)	-0.066	0.12	0.13	0.91	-0.140	0.12	0.12	0.75
	γ_1 (−0.8)	0.047	0.18	0.18	0.96		n.a.		
	γ_2 (0.5)	0.014	0.09	0.09	0.96		n.a.		
	θ_u (1.5)	-0.031	0.16	0.21	0.84	-0.700	0.30	0.20	0.32
	θ_v (1.5)	-0.034	0.16	0.18	0.89		n.a.		
	ρ (0.9)	0.003	0.01	0.01	0.89		n.a.		
Set 3	β_1 (−0.6)	0.054	0.22	0.22	0.95	0.247	0.20	0.21	0.75
	β_2 (0.8)	-0.060	0.12	0.12	0.91	-0.174	0.10	0.11	0.61
	γ_1 (−0.8)	0.054	0.18	0.18	0.94		n.a.		
	γ_2 (0.5)	0.013	0.09	0.09	0.95		n.a.		
	θ_u (2.0)	-0.051	0.27	0.32	0.86	-1.100	0.25	0.20	0.01
	θ_v (2.0)	-0.021	0.28	0.31	0.90		n.a.		
	ρ (0.95)	0.004	0.01	0.01	0.84		n.a.		
Set 4	β_1 (−0.6)	0.017	0.36	0.36	0.96	0.026	0.36	0.36	0.95
	β_2 (0.8)	-0.029	0.18	0.18	0.95	-0.034	0.18	0.18	0.94
	γ_1 (−0.8)	0.011	0.25	0.24	0.97		n.a.		
	γ_2 (0.5)	0.015	0.13	0.12	0.97		n.a.		
	θ_u (0.8)	0.030	0.06	0.15	0.89	-0.143	0.68	0.26	1.00
	θ_v (0.8)	-0.001	0.06	0.04	0.99		n.a.		
	ρ (0.2)	0.047	0.05	0.10	0.83		n.a.		
Set 5	β_1 (−0.6)	0.046	0.28	0.27	0.94	0.105	0.27	0.27	0.92
	β_2 (0.8)	-0.039	0.14	0.14	0.93	-0.074	0.14	0.14	0.90
	γ_1 (−0.8)	0.022	0.19	0.18	0.96		n.a.		
	γ_2 (0.5)	0.019	0.10	0.09	0.95		n.a.		
	θ_u (0.8)	0.044	0.07	0.13	0.89	-0.202	0.43	0.19	1.00
	θ_v (0.8)	0.033	0.07	0.09	0.92		n.a.		
	ρ (0.8)	0.009	0.02	0.02	0.89		n.a.		
Set 6	β_1 (−0.6)	0.002	0.26	0.25	0.95	0.031	0.25	0.25	0.96
	β_2 (0.8)	-0.037	0.13	0.12	0.96	-0.053	0.13	0.12	0.94
	γ_1 (−0.8)	0.014	0.18	0.18	0.95		n.a.		
	γ_2 (0.5)	0.010	0.09	0.09	0.95		n.a.		
	θ_u (0.8)	0.018	0.04	0.08	0.93	-0.170	0.51	0.20	1.00
	θ_v (0.8)	0.011	0.04	0.05	0.94		n.a.		
	ρ (0.8)	0.004	0.01	0.01	0.94		n.a.		